Discovery of a WZ Sge-Type Dwarf Nova, SDSS J102146.44+234926.3: Unprecedented Infrared Activity during a Rebrightening Phase

Makoto Uemura,[1] Akira Arai,[2] Tom Krajci,[3] Elena Pavlenko,[4] Sergei Yu. Shugarov,[5] Nataly A. Katysheva,[5]
Vitalij P. Goranskij,[5] Hiroyuki Maehara,[6] Akira Imada,[6] Taichi Kato,[6] Daisaku Nogami,[7] Kazuhiro Nakajima,[8]
Takashi Ohsugi,[1,2] Takuya Yamashita,[1] Koji S. Kawabata,[1] Osamu Nagae,[2] Shingo Chiyonobu,[2]
Yasushi Fukazawa,[2] Tsunefumi Mizuno,[2] Hideaki Katagiri,[2] Hiromitsu Takahashi,[2] Atsushi Ueda,[2]
Takehiro Hayashi,[9] Kiichi Okita,[10] Michitoshi Yoshida,[10] Kenshi Yanagisawa,[10] Shuji Sato,[11]
Masaru Kino,[11] and Kozo Sadakane[12]

[1]*Astrophysical Science Center, Hiroshima University, 1-3-1 Kagamiyama, Higashi-Hiroshima, Hiroshima 739-8526*
uemuram@hiroshima-u.ac.jp
[2]*Department of Physical Science, Hiroshima University, 1-3-1 Kagamiyama, Higashi-Hiroshima, Hiroshima 739-8526*
[3]*P.O. Box 1351, Cloudcroft, NM 88317, USA*
[4]*Crimean Astrophysical Observatory, Crimea, Nauchnyj, Ukraine*
[5]*Sternberg Astronomical Institute, Moscow, Russia*
[6]*Department of Astronomy, Faculty of Science, Kyoto University, Sakyo-ku, Kyoto 606-8502*
[7]*Hida Observatory, Kyoto University, Kamitakara, Gifu 506-1314*
[8]*VSOLJ, 124 Isatotyo Teradani, Kumano, Mie 519-4673*
[9]*Department of Education, Hiroshima University, 1-1-1 Kagamiyama, Higashi-Hiroshima, Hiroshima 739-8524*
[10]*Okayama Astrophysical Observatory, National Astronomical Observatory of Japan, Kamogata, Okayama 719-0232*
[11]*Department of Physics, Nagoya University, Furo-cho, Chikusa-ku, Nagoya 464-8602*
[12]*Astronomical Institute, Osaka Kyoiku University, Asahigaoka, Kashiwara, Osaka 582-8582*

Abstract

Several SU UMa-type dwarf novae and WZ Sge-type stars tend to exhibit rebrightenings after superoutbursts. The rebrightening phenomenon is problematic for the disk instability theory of dwarf novae, since it requires a large amount of remnant matter in the disk, even after superoutbursts. Here, we report on our optical and infrared observations during the first-ever outburst of a new dwarf nova, SDSS J102146.44 + 234926.3. During the outburst, we detected superhumps with a period of 0.056281 ± 0.000015 d, which is typical for superhump periods in WZ Sge stars. In conjunction with the appearance of a long-lived rebrightening, we concluded that the object is a new member of WZ Sge stars. Our observations, furthermore, revealed infrared behaviors for the first time in the rebrightening phase of WZ Sge stars. We discovered prominent infrared superhumps. We calculated the color temperature of the infrared superhump source to be 4600–6400 K. These temperatures are too low to be explained by a fully ionized disk appearing during dwarf-nova outbursts. We also found a K_s-band excess over the hot disk component. These unprecedented infrared activities provide evidence for the presence of mass reservoir at the outermost part of the accretion disk. We propose that a moderately high mass-accretion rate at this infrared active region leads to the long-lived rebrightening observed in SDSS J102146.44 + 234926.3.

Key words: accretion, accretion disks — stars: individual (SDSS J102146.44 + 234926.3) — stars: novae, cataclysmic variables

1. Introduction

Dwarf novae are a sub-class of cataclysmic variables that contain a Roche-lobe filling secondary star and an accreting white dwarf (for a review, see Warner 1995a). Dwarf nova outbursts are characterized with amplitudes of 2–5 mag and durations of a few days. SU UMa-type stars are dwarf novae showing two types of outbursts: normal outbursts and superoutbursts, which have longer durations (~ 10–20 d) and amplitudes of ~ 1 mag larger than those of normal outbursts. Superoutbursts are characterized by the appearance of periodic short-term modulations, called "superhumps", whose period is slightly longer than the orbital period (Warner 1995b).

Dwarf nova outbursts are caused by a sudden increase of the mass-accretion rate in an accretion disk. The most widely accepted theory for SU UMa stars is the thermal–tidal instability model for the accretion disk (Osaki 1989). The thermal-instability model considers two kinds of thermally stable states of the disk, that is, a cool disk of neutral hydrogen gas and a hot disk of ionized hydrogen gas, corresponding to the quiescent and outburst states, respectively. According to the disk instability model, the cool disk becomes thermally unstable when the density of the accumulated gas reaches a critical value. The disk then experiences a state transition to a hot disk, observed as an outburst (Osaki 1974; Hōshi 1979; Meyer & Meyer-Hofmeister 1981; Smak 1982; Cannizzo et al. 1982). The outburst leads to an expansion of the disk. In the case that the disk has sufficient angular momentum, its outer edge

reaches the 3:1 resonance radius, which triggers a tidal instability (Whitehurst 1988). The disk becomes eccentric, and as a result the strong tidal torque yields an additional dissipation of the angular momentum in the disk, which leads to superoutbursts. Because of the eccentricity of the disk, periodic modulations associated with the orbital motion of the secondary star are expected. They are actually observed as superhumps. The superhump period is longer than the orbital period due to the precession of the eccentricity wave (Patterson et al. 2005).

The disk instability model can explain several basic behaviors of ordinary dwarf novae, for example their frequency of outbursts and two kinds of outbursts in SU UMa stars (for a review, see Osaki 1996). This standard model is, however, required to be modified in order to reproduce rebrightenings after superoutbursts, which are observed in several SU UMa stars. A peculiar subclass, WZ Sge-type dwarf novae, in particular, tend to exhibit various types of rebrightenings (Howell et al. 1995; Kato et al. 2001). WZ Sge-type stars have the shortest orbital periods ($P_{orb} \sim 85$ min) and longest outburst cycles ($\gtrsim 10$ yr) among dwarf novae. Based on the characteristics of light curves, rebrightenings can be divided into three types: (i) a single short rebrightening (RZ Leo: Ishioka et al. 2001; ASAS J002511 + 1217.2: Templeton et al. 2006), (ii) repetitive short rebrightenings, or sometimes called "echo outbursts" (WZ Sge: Patterson et al. 2002; EG Cnc: Patterson et al. 1998, Kato et al. 2004; SDSS J080434.20 + 520349.2: Pavlenko et al. 2007), and (iii) a long-lived plateau (AL Com: Nogami et al. 1997, Ishioka et al. 2002; CG CMa: Kato et al. 1999; TSS J022216.4 + 412259.9: Imada et al. 2006a; V2176 Cyg: Novák et al. 2001). Additionally to WZ Sge stars, several short-period SU UMa stars also exhibit single or a few short rebrightenings (Baba et al. 2000; Uemura et al. 2002; Imada et al. 2006b). On the other hand, several WZ Sge stars show no sign of rebrightenings (HV Vir: Kato et al. 2001).

The mechanism of rebrightenings and the origin of their diversity are poorly understood. In a simple picture based on the disk-instability model, most of the mass and angular momentum are lost from the disk by the end of superoutbursts (Osaki 1996). The long-lived rebrightening phase is problematic because it apparently requires an unknown delayed mass-accretion, even after the termination of superoutbursts when the disk should be nearly empty (Kato et al. 2004). This discrepancy can be reconciled if the mass-transfer rate from the secondary is enhanced due to irradiation by the disk (Warner 1998; Hameury et al. 2000; Patterson et al. 2002). This scenario, however, has a difficulty to reproduce a sudden onset and cessation of the rebrightening phase (Patterson et al. 2002; Osaki & Meyer 2003, 2004). Kato et al. (1998) proposed an alternative scenario, in which a considerable amount of matter which is left over the 3:1 resonance radius is responsible for the delayed accretion. The remnants at the outermost region are expected to work as a mass reservoir, leading to additional mass accretion during the rebrightening phase (Hellier 2001; Osaki et al. 2001; Kato et al. 2004).

Hence, the behavior of the outermost region of the accretion disk definitely provides crucial clues for the rebrightening phenomenon. Infrared (IR) observations can be a strong tool to detect variations from a low-temperature region at the outermost accretion disk. Such IR observations during the
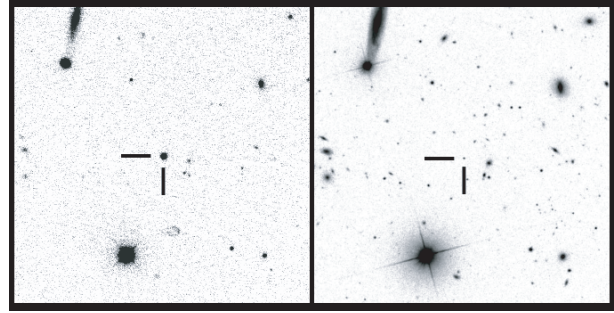

Fig. 1. Optical images of the field of J1021 in SDSS DR5 (right panel; Adelman-McCarthy et al. 2007) and observed with the KANATA 1.5-m telescope (left panel). The field of view is approximately $5' \times 5'$. J1021 is the object marked with the black bars.

rebrightening phase have, however, been difficult because of the low frequencies of outbursts of WZ Sge stars.

Here, we report on the results of our observations of a new variable star, which was a promising candidate for a WZ Sge star. The discovery of its outburst was reported by Christensen in 2006 November (Christensen 2006). There is a quiescent counterpart, SDSS J102146.44 + 234926.3 (hereafter, J1021) in the Sloan Digital Sky Survey (SDSS) DR5 database with magnitudes of $g = 20.74$ and $r = 20.63$ (Adelman-McCarthy et al. 2007). We conducted an international campaign for J1021, in which we succeeded to perform IR time-series observations during a rebrightening phase for the first time. In the next section, we describe our photometric observations. In section 3, the results of our observations are presented. In section 4, we discuss the results and the nature of the rebrightening phenomenon. In the final section, we summarize our findings.

2. Observations

Simultaneous optical and IR observations were performed with TRISPEC, attached to the KANATA 1.5-m telescope at Higashi-Hiroshima Observatory. TRISPEC is a simultaneous imager and spectrograph with polarimetry covering both optical and near-infrared wavelengths (Watanabe et al. 2005). We used the imaging mode of TRISPEC with V, J, and K_s filters. The effective exposure times for each frame were 63, 60, and 54 s in the V, J, and K_s bands, respectively. An example of the images is shown in the left panel of figure 1. The figure also includes an image of the same field in the SDSS DR5 database in the right panel for a comparison (Adelman-McCarthy et al. 2007). J1021 is the object marked with the black bars.

After making dark-subtracted and flat-fielded images, we measured the magnitudes of J1021 and comparison stars using a Java-based aperture photometry package. The V, J, and K_s magnitudes of J1021 were calculated from those of the comparison star located at R.A. = $10^h 21^m 53\overset{s}{.}33$, Dec = $+23°50'55\overset{''}{.}9$ ($V = 12.84$, $J = 12.22$, $K_s = 12.04$). We quote the V-band magnitude of the comparison star listed in the Henden's sequence[1] and the J and K_s-band magnitudes from the

---

[1] ⟨ftp://ftp.aavso.org/public/calib/varleo06.dat⟩.

Table 1. Observation log.

Site	Telescope	Camera	Filter	Date (+JD2454000)
Higashi-Hiroshima Astr. Obs.	KANATA 1.5-m	TRISPEC	V, J, K_s, none (optical channel)	70, 71, 74, 75, 76, 85, 88, 89, 91, 92, 100, 115, 123, 125, 126, 127, 130
Cloudcroft	28-cm	SBIG ST-7	none	60, 61, 62
Crimean Laboratory of SAI	50- and 60-cm	AP 47p	V, R_c	62, 63, 64, 65, 66, 69, 72, 73, 75, 76, 77, 79, 80, 81, 82, 84, 86, 90, 91
Crimean Astr. Obs. (CrAO)	2.6-m	FLI 1001E	R_c	91
Saitama	25-cm	SBIG ST-7XME	clear	61, 65, 71, 75
Kyoto Univ.	40-cm	SBIG ST-9	none	73, 74
Mie	25-cm	MUTOH CV04	none	73, 74, 75

2MASS catalog (Skrutskie et al. 2006). We checked the constancy of the comparison star using neighbor stars, and found that it exhibited no significant variations over 0.02, 0.03, and 0.06 mag in the V, J, and K_s-bands, respectively. For V- and J-band observations, we obtained time-series data that allowed us to study short-term variations in a night. For K_s-band observations, we only obtained averaged data for each night.

We also performed optical photometric observations with other telescopes during the period of JD 2454060–2454130 at 6 sites: Cloudcroft, Crimea, Saitama, Kyoto, and Mie. Details of their observational equipment are summarized in table 1. The magnitude systems with a clear filter or without any filters were adjusted to the V-band observation by TRISPEC/KANATA by adding constants.

3. Results

3.1. Overall Behavior of the 2006 Outbursts of J1021

According to Christensen (2006), J1021 had already been in outburst on JD 2454037 with $V = 13.9$. We confirmed the outburst on JD 2454060, 23 d after the first record of the outburst. Our observation campaign then started, revealing the overall behavior of the outburst and a subsequent fading phase, as shown in figure 2. Panel (a) includes all observations from the discovery to a fading phase from the outburst. The event can be divided into 5 phases: the main outburst (JD 2454037–2454065), the dip (JD 2454066–2454067), the rebrightening (JD 2454068–2454077), the rapid fading phase (JD 2454079–2454081), and the long fading tail (JD 2454082–).

The total duration from the main outburst to the rebrightening was at least 40 d. The average fading rate was 0.05 mag d^{-1} during the main outburst. Compared with typical durations of superoutbursts (10–15 d: Warner 1995a), the total duration is atypically long. It is rather reminiscent of WZ Sge stars, whose total duration of outbursts (including rebrightening phases) is 60–100 d (Kato et al. 2001).

The main outburst was terminated by the dip, whose duration is $\lesssim 3$ d. The object, then, experienced a rebrightening. Panel (b) of figure 2 shows light curves during the main outburst, the dip, and the rebrightening phase. The rebrightening continued for 10–11 d. These features of the light curve are quite analogous to the dip–long-lived plateau structure observed in several WZ Sge stars, that is, AL Com, CG CMa, TSS J022216.4 + 412259.9, and V2176 Cyg (Nogami et al. 1997; Ishioka et al. 2002; Kato et al. 1999; Imada et al. 2006a; Novák et al. 2001).

The object entered a rapid fading phase from the rebrightening on JD 2454079. The rapid fading stopped at 2.4 mag brighter than its quiescence. The object then exhibited a long fading tail. It took at least 50 d until returning to its quiescent level. This long fading is also one of characteristics observed in WZ Sge stars (Kato et al. 2004). Ordinary SU UMa stars return to their quiescent level within a few days after superoutbursts.

3.2. Rising Phase of the Rebrightening

We found that the rising trend to the rebrightening maximum was not monotonous. The rebrightening was first observed for JD 2454068. With the observation on JD 2454067, the rising rate was calculated to be < -1.2 mag d^{-1}. The rising trend apparently became weak, or stopped between JD 2454068–2454069, as can be seen from the figure 2. We detected a clear brightening trend, -0.47 ± 0.06 mag d^{-1}, in the data on JD 2454069. The object then reached the rebrightening maximum on JD 2454070. The rapid rising trend was thus temporarily terminated on JD 2454068, and restarted on JD 2454069.

Similar structures in light curves were also observed in other WZ Sge stars showing long plateau-type rebrightenings. In the case of the 1995 outburst of AL Com, a rapid rising from the dip was followed by a temporary fading. As a result, a clear precursor appeared just before the rebrightening maximum (Nogami et al. 1997). In the case of V2176 Cyg, we can see a clear fading trend in the first day of a rebrightening (Novák et al. 2001). This feature also indicates the presence of a precursor before the rebrightening maximum.

The observed structure in J1021 can also be interpreted as being a sign of a precursor before the rebrightening maximum. These precursors may be a common characteristic in long plateau-type rebrightenings in WZ Sge stars. The durations
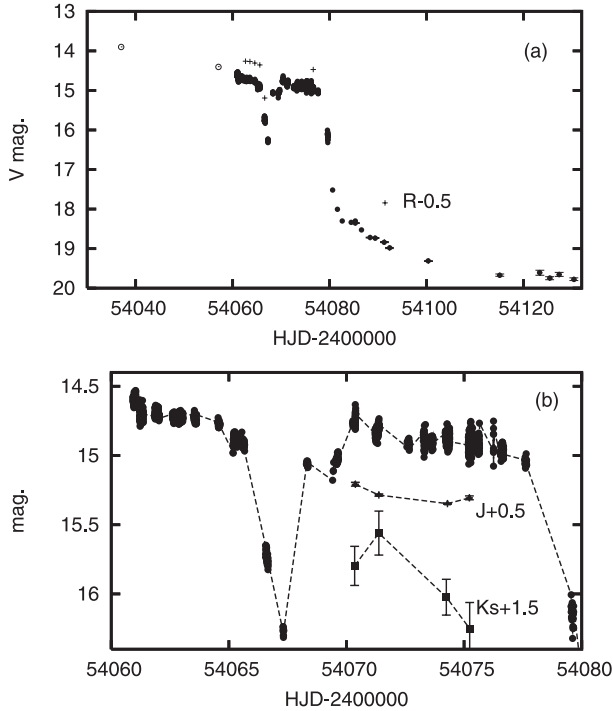
Fig. 2. Light curves of the outburst of J1021 in 2006. The abscissa and ordinate denote the time in HJD and the magnitude, respectively. (a) Whole light curve of the outburst. The filled circles are our V-band and unfiltered CCD observations. The crosses are one-day averages of R_c-magnitudes, which are shifted by adding -0.5 mag, as indicated in the figure. The open circles represent the V-band observations reported in Christensen (2006). (b) Enlarged light curve of the main outburst, the dip, and the rebrightening phase. The filled triangles and squares are J- and K_s-bands observations, respectively. These infrared points are averaged magnitudes of each night. The magnitudes of the infrared points are shifted in this figure by adding constants of 0.5 mag (J) and 1.5 mag (K_s), as indicated in the figure.

of the precursors are < 2 d in all cases, which also supports the scenario that the observed precursors have the same nature.

3.3. Color Variations

We performed simultaneous V- and R_c-band observations, as shown in the panel (a) of figure 2. Using these data, we show temporal variations of the color $V - R_c$ in the upper panel of figure 3. The object first remained at $V - R_c = -0.04$ during the main outburst, then slightly reddened to $V - R_c = +0.04$ just before the rapid fading stage. During the rebrightening phase, it again became bluer ($V - R_c = -0.01$). A quite red color was observed during the long fading tail ($V - R_c = +0.49$).

Our observations revealed the IR behavior of WZ Sge stars during a rebrightening phase for the first time. The J- and K_s-band light curves are shown in the panel (b) of figure 2. The J-band light curve follows a temporal evolution similar to the optical one, that is, a gradual fading trend since the rebrightening maximum and a slightly brightening at $\sim$ JD 2454075. The K_s-band light curve, in contrast to the J-band one, the maximum apparently delayed to the optical one, which is followed by a rather rapid fading. As a result, the color variations also show different behaviors between $V - J$ and $J - K_s$,
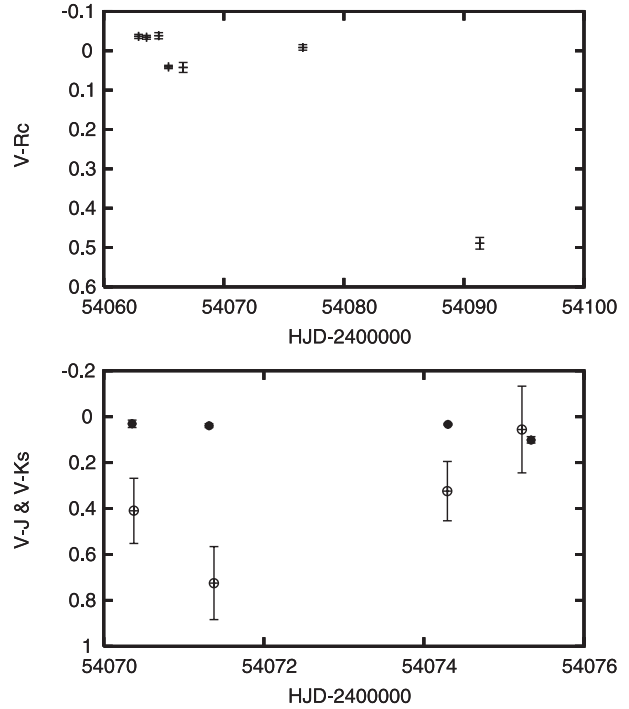

Fig. 3. Temporal color variations. The abscissa and ordinate denote the time in HJD and the color indices. Upper panel: variations of $V - R_c$. Lower panel: variations of $V - J$ and $J - K_s$. The filled and open circles are $V - J$ and $J - K_s$, respectively.

as can be seen in the lower panel of figure 3. As reported in subsections 3.4 and 3.5, there are periodic short-term humps in the light curves. The colors in figure 3 were calculated from the magnitudes at the bottom of the humps in order to avoid the contribution from the variable hump component.

As can be seen in figure 3, the color index of $V - J$ almost remains constant at ~ 0.03 in JD 2454070–2454075. The color $J - K_s$, on the other hand, exhibits dramatic variations from $J - K_s = 0.7$ to 0.1. The $V - J$ color during the rebrightening is typical for the color of dwarf novae in outburst ($B - V \sim 0$: Bailey 1980).

Spectra during dwarf nova outbursts are described with the multi-temperature blackbody model (or the standard disk model: Shakura & Sunyaev 1973). The temperatures of the disk in dwarf nova outbursts are from $\sim 10^5$ K to $\sim 10^4$ K at the innermost and outermost region, respectively (e.g., Horne & Cook 1985). Thus emission between the V- and J-bands originates from the outermost region of the disk. As a result, this region of the spectra can be well described with a simple blackbody spectrum. We corrected the interstellar reddening for the observed color $V - J$ using the maximum reddening for the direction of J1021, expected to be $E(V - J) = 0.05$ based on the database in Schlegel et al. (1998). In the case of J1021 in the rebrightening phase, the intrinsic color $V - J = 0.08$ indicates a color temperature of 9000 K. The blackbody approximation is also supported by the blue color of $V - R_c = -0.01$ during the rebrightening phase.

Figure 4 shows the temporal development of spectral energy distributions (SED) during the rebrightening phase. The filled circles are our V-, J-, and K_s-band observations. The dashed
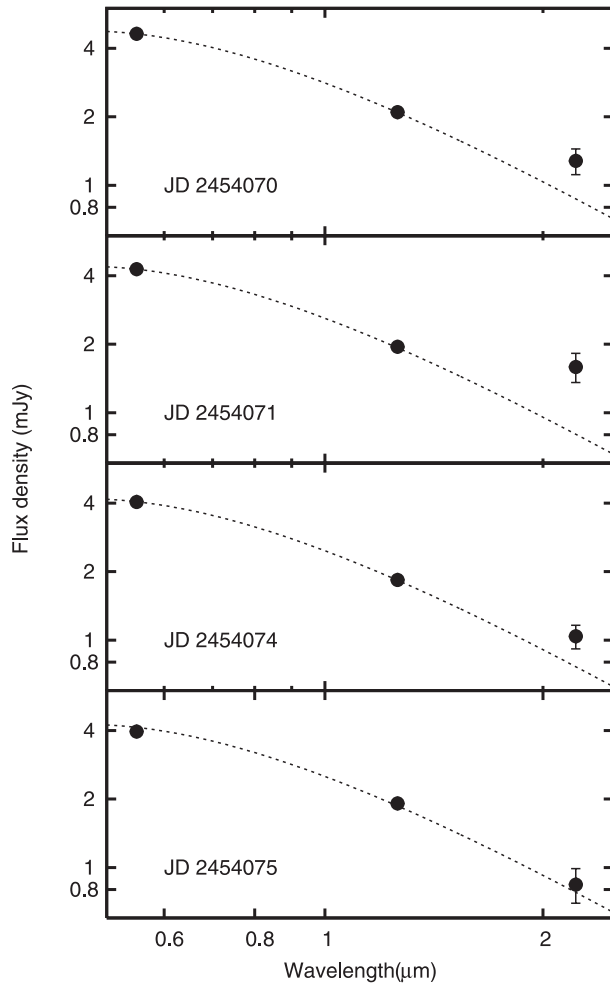
Fig. 4. Spectral energy distributions between the V- and K_s-bands during rebrightening. The abscissa and ordinate denote the wavelength in μm and the flux density in mJy, respectively. The figure has 4 panels for each observation date, that is, JD 2454070, 2454071, 2454074, and 2454075. The filled circles are our V-, J-, and K_s-band observations. The dashed lines indicate a blackbody spectrum with a temperature of 9000 K.

lines indicate a blackbody spectrum with a temperature of 9000 K. As can be seen in the figure, there are significant excesses in the K_s-band flux over the blackbody spectrum. The excess reached the maximum at JD 2454071, and then, rapidly decreased with time. In JD 2454075, there is no significant excess in the K_s-band, and the SED can be described by a the simple blackbody in the V-, J-, and K_s-bands regime. These results strongly indicate the appearance of another emission source outside the high-temperature disk. This component was dominant at wavelengths longer than $\sim 2\,\mu$m for the first couple of days of the rebrightening, and then disappeared on a time-scale of a few days.

3.4. Temporal Evolution of Optical Superhumps

We detected short-term periodic modulations during the outburst. Examples of them are shown in figure 5. They have common characteristics of $\lesssim 0.1$ mag amplitudes, except for those observed during the early fading tail, which have larger

amplitudes of 0.3–0.4 mag. During the main outburst, they have clear sawtooth profiles, which are typical for superhumps in SU UMa-type dwarf novae in a superoutburst.

We calculated the periods of the modulations in the main outburst, the rebrightening phase, and the fading tail. We performed period analysis using the Phase Dispersion Minimization (PDM) method (Stellingwerf 1978) for the data during the main outburst (JD 2454060–2454065), the rebrightening phase (JD 2454068–2454077), and the fading tail (JD 2454082–2454091). Note that our sample of the fading tail only covers its early phase. Using those data, we calculated the Θ defined in the PDM method for each frequency. The obtained frequency–Θ diagrams are shown in figure 6. The best periods were calculated to be $P_{\mathrm{main}} = 0.056281 \pm 0.000015$ d, $P_{\mathrm{rebr}} = 0.056283 \pm 0.000018$ d, and $P_{\mathrm{tail}} = 0.055988 \pm 0.000015$ d for the main outburst, the rebrightening, and the fading tail, respectively. The period in the main outburst is in agreement with that in the rebrightening within the errors, while P_{tail} is significantly shorter than those periods. These short periods are typical for superhump periods in WZ Sge stars. In conjunction with the appearance of the long-lived rebrightening and the fading tail, we conclude that J1021 is a new member of WZ Sge stars (also see, Golovin et al. 2007). The superhump period of J1021 is hence $P_{\mathrm{SH}} = P_{\mathrm{main}} = P_{\mathrm{rebr}}$.

In the case of J1021, we can find no sign of early superhumps, which are known as the most convincing evidence for the WZ Sge nature (Kato et al. 2004). The lack of early superhumps is naturally explained because they appear only in the first week of the main outburst, in which we had no time-series data in J1021.

Figure 7 presents the temporal evolution of superhumps. The light curves are folded with P_{SH} for each night. As can be seen from the figure, the superhump amplitude decreased with time during the main outburst (JD 2454060–2454064, labeled "60", "62", and "64" in the figure). The superhump profiles consist of the main hump at the phase ~ 0 and a secondary hump at the phase ~ 0.5, which is a typical characteristic for the late-phase of superoutbursts in ordinary SU UMa stars (Patterson et al. 2003). During the rapid fading phase from the main outburst, the phase of humps were apparently inverted ("66"), while this trend was not confirmed in later observations ("67"). We can only find a sign of modulations during the dip. The superhump signal then weakened during the precursor and just before the precursor maximum ("68" and "69"). An regrowth of superhumps was observed at the precursor maximum. Their profile and phase are quite analogous to those observed during the main outburst, having the main and secondary humps ("70"). The profile changed to a flat-top one in the late rebrightening phase, while their overall phase apparently remained unchanged ("72" and "75").

As mentioned above, a significantly shorter periodicity was found in the early fading tail. The averaged profile of the short-term modulations is shown in figure 8. The most noteworthy feature of the modulations is a large amplitude of ~ 0.2 mag compared with those in the superhumps during the superoutburst.

It is well known that superhump periods tend to increase throughout superoutbursts of WZ Sge stars (Kato et al. 2001).
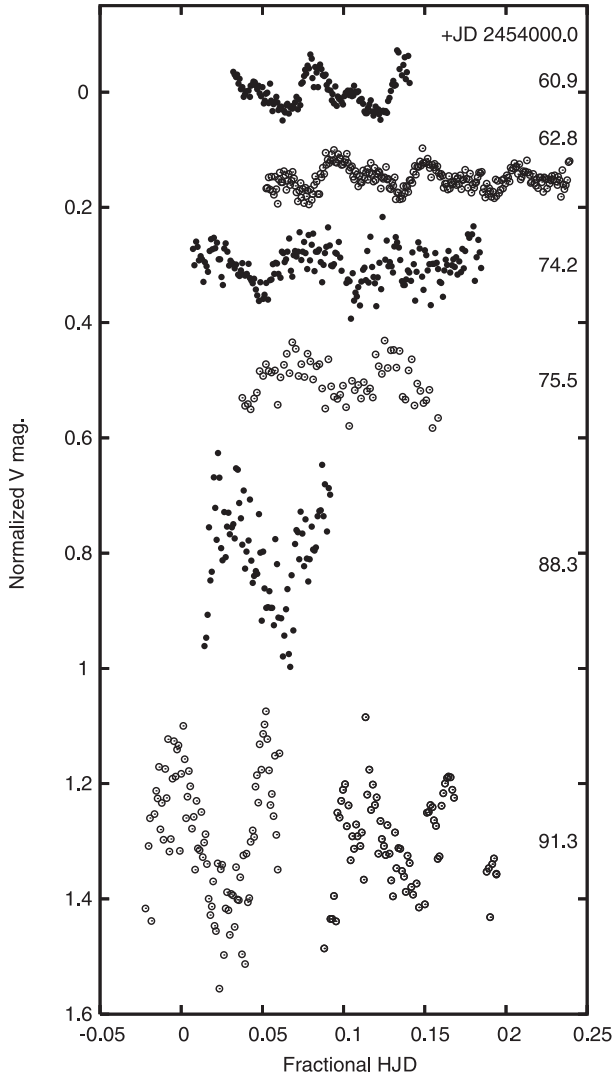
Fig. 5. Examples of short-term variations during the main outburst (JD 2454060 and 2454062), the rebrightening phase (JD 2454074 and 2454075), and the fading tail (JD 2454088 and 2454091). The abscissa and ordinate denote the fractional HJD and the V-band magnitudes, respectively. The magnitudes are normalized by their averages and shifted by constants.

Fig. 6. Frequency–Θ diagrams of superhumps in J1021. The abscissa and ordinate denote the frequency in d^{-1} and the Θ defined in the PDM method (Stellingwerf 1978). The panels of (a), (b), and (c) present the results calculated by the data in the main outburst, the rebrightening phase, and the fading tail, respectively.

In order to search possible variations of the superhump period in J1021, we determined the peak times of observed superhumps. The peak times were calculated by taking cross-correlations between the observed light curves and templates of superhump profiles. The templates are averaged profiles during the main outburst, the rebrightening phase, and the fading tail. Using the determined peak times of the superhumps, we calculated their $O-C$s values with the period of $P_{\rm SH}$ and the epoch of HJD 2454060.979634, the first superhump maxima that we observed. As a result, we obtained the $O-C$ diagram depicted in figure 9. The superhumps maintained a constant $O-C$ until the rebrightening maximum. A fitting of a quadratic curve for $O-C$s between the cycle 0 and 200 yielded no significant period derivative [$\dot{P}/P = (2.1 \pm 2.5) \times 10^{-6}$]. In figure 9, the $O-C$ apparently jumped during the rebrightening phase. As can be seen from figure 7, this is attributed not to the phase shift
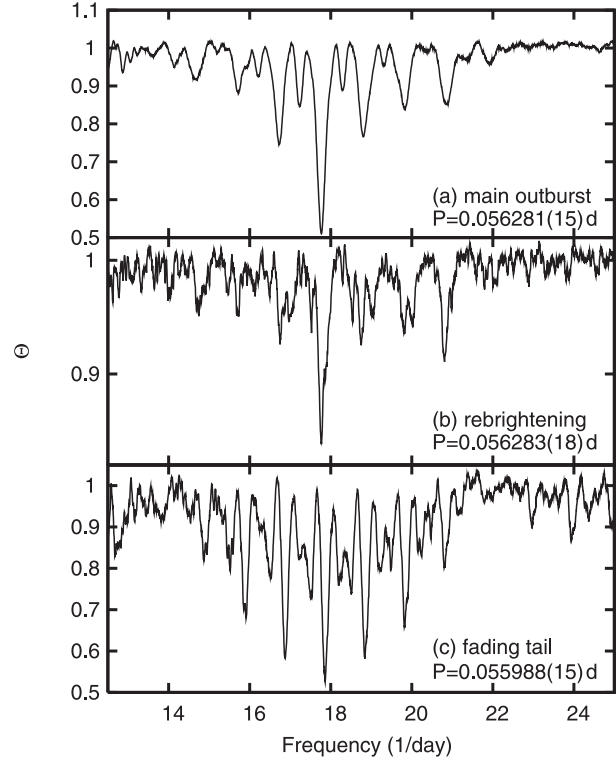
of overall superhumps, but to the variation of the superhump profile and the peak phase of the superhumps. We confirm the shorter periodicity in the early fading tail in figure 9.

3.5. Infrared Superhumps during the Rebrightening Phase

We succeeded to obtain simultaneous V- and J-band light curves of superhumps on JD 2454074 and 2454075 during the rebrightening phase. Figure 10 presents superhump profiles in the V- and J-bands. The superhump amplitude in the J-band is significantly larger than that in the V-band. Between JD 2454074 and 2454075, the J-band superhumps, furthermore, evolved in amplitude. A clear double-peak profile is seen in the superhumps on JD 2454075, and a hint of the same profile can also be seen on JD 2454074. The phases of these double peaks are apparently in agreement with those of the optical superhumps observed during the main outburst and the early phase of the rebrightening, as can be seen from figure 7. These unprecedented "IR superhumps" indicate that the superhump source releases its energy not mainly in the optical, but in the IR regimes.

In previous multicolor optical observations, the color at the superhump maxima is only slightly redder than that at the bottom of the superhumps (Stolz & Schoembs 1984; Hassall 1985; Bruch et al. 1996). The superhump temperature has been estimated to be 6000–10000 K, which is considered to be the temperature at the outermost region of the accretion disk in an outburst. On the other hand, Smak (2005) has recently
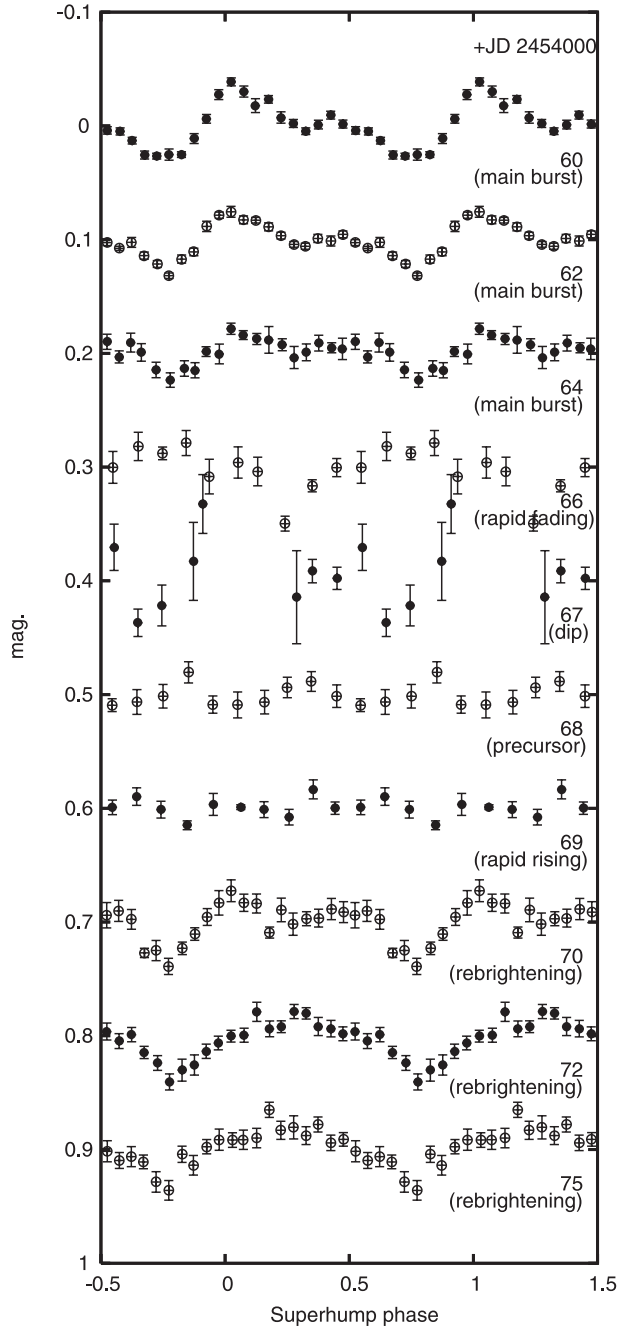
Fig. 7. Phase-averaged light curves of superhumps. The abscissa and ordinate denote the superhump phase and the differential magnitude, respectively. The superhump phase is defined by $P_{\rm SH} = 0.056281$ d and an arbitrary epoch. The light curves are normalized by their average magnitudes for each night and shifted to be readily compared. The observation dates and states during the outburst are also indicated in the figure.

Fig. 8. Phase-averaged light curves of the humps observed during the fading tail. The symbols are the same as in figure 7, except for the hump period for folding the light curve (0.055988 d).

Fig. 9. $O - C$ diagram of superhumps in J1021. The abscissa and ordinate denote the cycle of superhumps and the $O - C$ in days, respectively. The corresponding phases are also indicated in the figure.

suggested that a higher temperature ($\gtrsim 15000$ K) is theoretically required for superhump sources.

In order to estimate the temperature of the IR superhump source in J1021, we considered two components of blackbody emissions, that is, a variable (superhump) component and an invariable inner disk component. We calculated the color tempe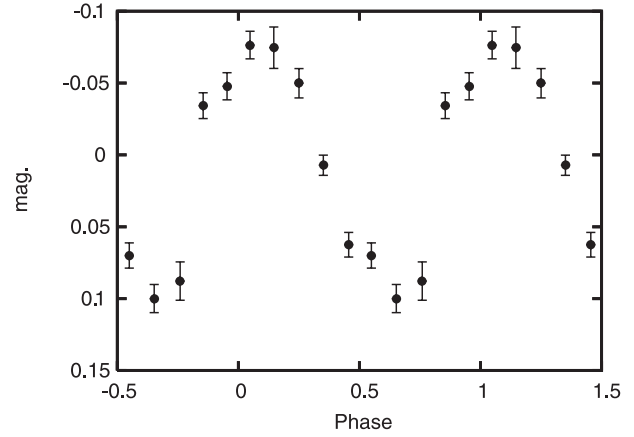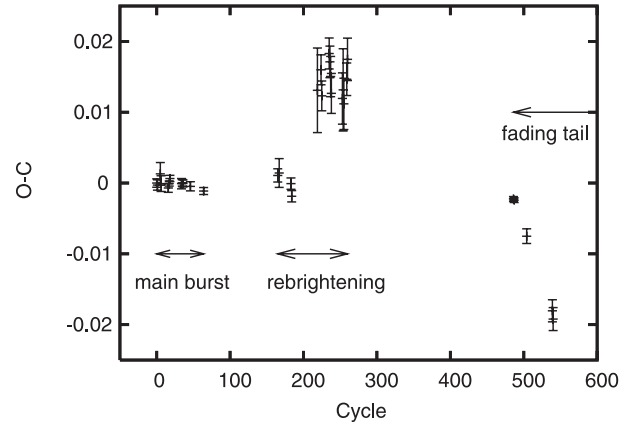ratures for each component. The color temperature of the invariable component was determined from the $V - J$ color at the bottom of the superhumps. Using this color temperature, we could calculate the color temperature and the size of the emitting area of the variable component from the V- and J-band amplitudes of the superhumps. The size of the emitting area of the variable component is a relative one to that of the invariable component. The interstellar reddening was corrected, as mentioned above.

The results are summarized in table 2. The temperature of the invariable component ($T_{\rm base}$) is 9000 K on both dates, which is typical for the outermost region of accretion disks in outburst. The temperature of the variable component ($T_{\rm var}$) is, on the other hand, much lower than that of the invariable component. The evolution of the IR superhumps between JD 2454074 and 2454075 requires both a lower temperature and a larger emitting area. The temperature of 4600 K on JD 2454075 is atypically low compared with superhump temperatures previously reported in SU UMa stars. The large emitting area of the variable component on JD 2454075 is particularly remarkable. In conjunction with the constant
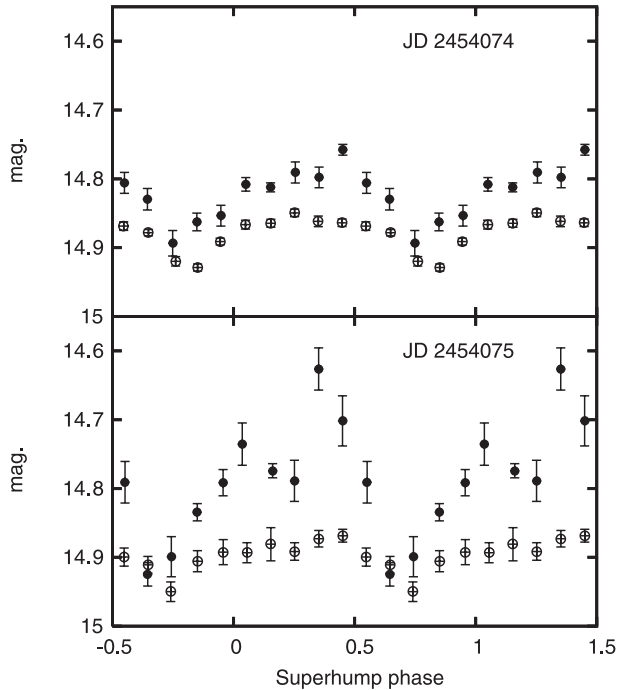
Fig. 10. Optical and IR superhump profiles during the rebrightening phase. The abscissa and ordinate denote the superhump phase and the V and J magnitude, respectively. The superhump phase is defined by the same period and epoch as in figure 7. The filled and open circles represent the J- and V-band superhumps, respectively. The upper and lower panels are observations on JD 2454074 and 2454075, respectively.

Table 2. Color temperatures of variable and invariable components.

JD	T_{base} (K)	T_{var} (K)	Emitting area*
2454074	9000 ± 300	6400 ± 400	0.3 ± 0.2
2454075	9000 ± 300	4600 ± 300	1.4 ± 0.4

* The emitting area of the variable component relative to that of the invariable one.

temperature and the magnitude of the invariant component, the evolution of the IR superhumps implies a rapid outward expansion of the IR superhump source from JD 2454074 to 2454075. In addition, the large relative emitting area of IR superhumps indicates that the actual size of the inner, invariable hot disk is small.

3.6. Active Low Temperature Region at the Outermost Part of Accretion Disks

As mentioned above, our observations of J1021 revealed unprecedented IR activities during the rebrightening phase, namely the K_s-band excess (subsection 3.3) and the IR superhumps (subsection 3.5). These results strongly indicate the presence of a cool component outside the hot inner disk during the rebrightening. Our detection of prominent IR superhumps, moreover, revealed that the outer disk is not only cool, but also active in terms of the tidal instability. Hence, the tidal dissipation still enhances the mass accretion in the outer disk. The observed IR superhumps require an extensive cool component

over the 3:1 resonance radius, which means that a substantial amount of matter is stored and active outside the hot inner disk.

The optical behavior of J1021 during the rebrightening phase is analogous to those previously observed in other WZ Sge stars (e.g., Nogami et al. 1997). There is no hint for the cool component only with the optical data of J1021. To date, optical observations during rebrightening phases have failed to find any clue for a mass reservoir outside the hot inner disk, while its presence has been expected (Kato et al. 1998; Hellier 2001; Osaki et al. 2001; Kato et al. 2004). The IR active region of J1021 finally provides evidence for the presence of the mass reservoir during the rebrightening phase. We propose that the strong tidal dissipation working at the cool active region maintains a moderately high mass-accretion rate at the outermost area, which sustains the hot state of the inner disk.

Patterson et al. (1998) reported an unusually red color of $V - I \sim 0.9$ and strong Na D absorption during the rebrightening phase of a WZ Sge star, EG Cnc. These features can be retrospectively interpreted as a hint of the extensive cool component in the outer disk, although the original authors implied a rather usual quiescent disk behind a cooling wave. We note that another hint of the cool component can be seen during the rebrightening phase of WZ Sge. According to Howell et al. (2004), at the rebrightening maximum of WZ Sge, the color temperatures derived from B-, V-, and R-band observations are 9000–10000 K, although the observed $R - I$ indicates only 7700 K. This implies an I-band excess over the ~ 10000 K disk. This can also be interpreted with a cool mass-reservoir. A sign of the cool component was also observed as deep Na D absorption lines during the main outburst of WZ Sge (Nogami & Iijima 2004).

In the theoretical framework of dwarf novae, state transitions between a cool and a hot disk must occur in an entire disk (Smak 1984; Mineshige & Osaki 1985). The temperature of the IR superhumps is, however, much lower than those permitted for a hot disk ($\gtrsim 8000$ K). Our observation of J1021 during rebrightening indicates that it had no entire hot disk, but had a two-component disk, namely a hot inner disk and a cool or transitional state disk at the outermost part. Such a simultaneous presence of hot and cool disks could be problematic for the thermal-instability model.

4. Discussion

4.1. Infrared Behavior during Dwarf Nova Outbursts in General

In the previous section, we reported on IR activity during the rebrightening phase of J1021. The uniqueness of its IR behavior among SU UMa stars is, however, unclear due to a lack of enough samples for IR observations during dwarf nova outbursts. Naylor et al. (1987) reported optical and IR observations during a superoutburst of an ordinary SU UMa-type dwarf nova, OY Car. In their paper, optical and IR superhumps have similar amplitudes: ~ 0.3 mag both in B- and J-bands. They are consistent with the classical picture of an accretion disk in dwarf nova outbursts, in which a superhump source having 8000–10000 K lies at the outermost part of the disk having $\gtrsim 10000$ K. The IR behavior of OY Car is totally different from that observed in the rebrightening phase

of J1021. To date, this observation of OY Car is all information about the IR behavior during superoutbursts. Regarding J1021, furthermore, we have no IR data during the main outburst, which should be compared with those during the rebrightening. In order to reveal the nature of the IR active region, future IR observations are required during superoutbursts and the rebrightenings of ordinary SU UMa and other WZ Sge stars.

4.2. Validity of the Color Temperature

In the previous section, we discussed our calculation of the color temperatures of superhump sources from the observed colors. As a result, we obtained low color temperatures, which were rather close to those observed at quiescence. The color temperature provides a good approximation if the source is optically thick. In dwarf novae, however, the optical light from the accretion disk at quiescence is, in general, dominated by optically thin emission (Howell et al. 2004, and references therein). Even in outbursts, the continuum radiation at the outermost region is predicted to be optically thin (Williams 1980). In the case of J1021 during rebrightening, the temperature of the IR superhumps was rather close to the quiescent one, although the entire disk luminosity was still high. The radiation mechanism of the IR superhumps is, hence, less obvious. If the IR emission is optically thin, the color temperatures of the low temperature region given in table 2 may have no complete validity as an indicator of real temperatures. We thus need to solve the radiation transfer in the disk in order to reproduce the observed light curves, which is, however, beyond the scope of this paper. The results of such a full calculation, on the other hand, have only little influence on our order-of-magnitude discussion. IR spectroscopic observations are required to conclude whether the outer low-temperature region is optically thin or thick during the rebrightening phase.

4.3. Delayed Maximum of Rebrightenings in WZ Sge Stars

Among 5 systems showing long plateau-type rebrightenings, 3 systems exhibit a precursor just before their rebrightening maximum, as mentioned in subsection 3.2. In ordinary SU UMa stars, precursors are occasionally observed just before supermaxima. They are interpreted as a normal outburst triggering a subsequent superoutburst (Osaki & Meyer 2003). After the precursor maximum, the object starts rapid fading, since it takes a few days for the full evolution of the tidal instability. When the tidal dissipation begins working effectively, the rapid fading is terminated by a rising trend toward the supermaximum. The similar mechanism may also work in the structure of the long plateau-type rebrightening.

Light curves between precursors and rebrightening maxima are, however, peculiar in WZ Sge stars compared with the precursor–supermaximum structure in ordinary SU UMa stars. Several WZ Sge stars keep a gradually rising trend after initial rapid risings of rebrightenings. AL Com and V2176 Cyg, for example, reached the maxima of rebrightenings ~ 5 and ~ 4 d after the precursors, respectively (Nogami et al. 1997; Novák et al. 2001). TSS J022216.4+412259.9 is an extreme case, in which a gradual rising apparently continued for ~ 8 d until the rebrightening maximum (Imada et al. 2006a). This characteristic is clearly different from that observed in ordinary superoutbursts in which objects reach their supermaxima within

a day after the onset of outbursts (Warner 1995b). Although J1021 shows no delay of the rebrightening maximum, we discuss the delayed maximum in terms of the mass reservoir at the outermost part of the disk.

According to the disk instability model, the rising speed corresponds to the propagation speed of the heating wave in the hot disk (Mineshige & Osaki 1985). The delayed rebrightening maximum can possibly be attributed to a late propagation of the heating wave into the outer mass reservoir, namely the IR-active region. If the IR superhumps observed in J1021 are a characteristic feature for the rebrightening phase, however, this scenario is unlikely, because it would yield an entire hot disk and prominent optical superhumps.

Another possible scenario for the delayed rebrightening maximum is that the inner hot disk continuously receives a sufficient amount of gas from the outer mass reservoir. In the case of J1021, the tidal dissipation works effectively at the outer low-temperature region, as demonstrated by the IR superhumps. We can, thus, naturally expect significant mass accretion from the outer cool part to the inner hot part of the disk.

4.4. Origin of the K_s-Band Excess

During the rebrightening phase, the K_s-band flux exhibited a clear excess over the blackbody component that dominated between the V and J ranges, as mentioned in subsection 3.3. A noteworthy feature of the K_s-band light curve is a relatively rapid evolution compared with V- and J-band ones. The V- and J-band emission is presumably dominated by optically thick emission from the disk. Their evolution time-scale is a viscous diffusion time-scale of the hot optically thick disk. The time-scale becomes longer in an outer, in other words, lower temperature region of the disk. The rapid evolution of the K_s-band emission is thereby inconsistent with the theory of an optically thick disk. It implies that the K_s-band emission is not from an optically thick disk, but an optically thin region that is located outside the optically thick disk. The source of the K_s-band emission might be expelled from the optically thick disk at the onset of the rebrightening as the result of a rapid expansion of the hot disk.

4.5. On the Nature of the Periodicity in the Early Fading Tail

The periodic modulations during the early fading tail has a slightly shorter period than the superhumps, as can be seen from figures 6 and 9. The nature of the shorter period modulations is unclear. The period is possibly the orbital period of J1021. If this is the case, the superhump excess, $\varepsilon = (P_{\mathrm{SH}} - P_{\mathrm{orb}})/P_{\mathrm{orb}}$, is calculated to be 0.0052 ± 0.0003. The empirical relationship between the ε and the mass ratio of binary systems reported in Patterson (2001) yields a mass ratio of $M_2/M_1 = 0.024$ for J1021. The ε and the mass ratio are the smallest ones among previously known dwarf novae (Patterson 2001). J1021 is possibly the most evolved dwarf nova if the period of the modulations in the fading tail indicates the orbital period. An alternative possibility is that they are late superhumps. Late superhumps are periodic modulations appearing just after superoutbursts (van der Woerd et al. 1988; Rolfe et al. 2001). Their period is in agreement with a superhump period, while their profile is ~ 0.5 phase shifted from that of superhumps. In the case of J1021, we cannot confirm a clear phase

shift in figure 9. We, however, consider that the late super-hump scenario is more plausible because the long fading tail indicates an effective tidal dissipation, in which we can expect a long-lived eccentric disk and the superhump periodicity. As can be seen in figure 9, the $O - C$s of humps are apparently changed smoothly from the main outburst to the rebrightening and the early fading tail. This also supports the late superhump scenario.

5. Summary

Our observation of J1021 detected superhumps with a period of 0.056281 ± 0.000015 d. The object experienced a long plateau-type rebrightening after the main superoutburst, which is observed only in WZ Sge-type dwarf novae. In conjunction with the short superhump period, we conclude that J1021 is a new member of WZ Sge stars. We, furthermore, revealed IR behaviors for the first time during rebrightening phases of WZ Sge stars. J1021 exhibited unprecedented IR activities,

namely the K_s-band excess and the IR superhump. The IR superhump, in particular, indicates the presence of a substantial amount of remnant matter at the outermost region of the accretion disk, even after the main superoutburst. We propose that this outer low-temperature region is responsible for maintaining a hot state of the inner disk during rebrightening.

References

Adelman-McCarthy, J. K., et al. 2007, VizieR Online Data Catalog, II/276, 0

Baba, H., Kato, T., Nogami, D., Hirata, R., Matsumoto, K., & Sadakane, K. 2000, PASJ, 52, 429

Bailey, J. 1980, MNRAS, 190, 119

Bruch, A., Beele, D., & Baptista, R. 1996, A&A, 306, 151

Cannizzo, J. K., Ghosh, P., & Wheeler, J. C. 1982, ApJ, 260, L83

Christensen, E. J. 2006, Cent. Bur. Electron. Telegrams, 746, 1

Golovin, A., et al. 2007, IBVS, 5763, 1

Hameury, J.-M., Lasota, J.-P., & Warner, B. 2000, A&A, 353, 244

Hassall, B. J. M. 1985, MNRAS, 216, 335

Hellier, C. 2001, PASP, 113, 469

Horne, K., & Cook, M. C. 1985, MNRAS, 214, 307

Hōshi, R. 1979, Prog. Theor. Phys., 61, 1307

Howell, S. B., Henden, A. A., Landolt, A. U., & Dain, C. 2004, PASP, 116, 527

Howell, S. B., Szkody, P., & Cannizzo, J. K. 1995, ApJ, 439, 337

Imada, A., et al. 2006b, PASJ, 58, 143

Imada, A., Kubota, K., Kato, T., Nogami, D., Maehara, H., Nakajima, K., Uemura, M., & Ishioka, R. 2006a, PASJ, 58, L23

Ishioka, R., et al. 2001, PASJ, 53, 905

Ishioka, R., et al. 2002, A&A, 381, L41

Kato, T., Matsumoto, K., & Stubbings, R. 1999, IBVS, 4760

Kato, T., Nogami, D., Baba, H., & Matsumoto, K. 1998, in ASP Conf. Ser. 137, Wild Stars in the Old West, ed. S. Howell, E. Kuulkers, & C. Woodward (San Francisco: ASP), 9

Kato, T., Nogami, D., Matsumoto, K., & Baba, H. 2004, PASJ, 56, S109

Kato, T., Sekine, Y., & Hirata, R. 2001, PASJ, 53, 1191

Meyer, F., & Meyer-Hofmeister, E. 1981, A&A, 104, L10

Mineshige, S., & Osaki, Y. 1985, PASJ, 37, 1

Naylor, T., Charles, P. A., Hassall, B. J. M., Bath, G. T., Berriman, G., Warner, B., Bailey, J., & Reinsch, K. 1987, MNRAS, 229, 183

Nogami, D., & Iijima, T. 2004, PASJ, 56, S163

Nogami, D., Kato, T., Baba, H., Matsumoto, K., Arimoto, J., Tanabe, K., & Ishikawa, K. 1997, ApJ, 490, 840

Novák, R., Vanmunster, T., Jensen, L. T., & Nogami, D. 2001, IBVS, 5108, 1

Osaki, Y. 1974, PASJ, 26, 429

Osaki, Y. 1989, PASJ, 41, 1005

Osaki, Y. 1996, PASP, 108, 39

Osaki, Y., & Meyer, F. 2003, A&A, 401, 325

Osaki, Y., & Meyer, F. 2004, A&A, 428, L17

Osaki, Y., Meyer, F., & Meyer-Hofmeister, E. 2001, A&A, 370, 488

Patterson, J. 2001, PASP, 113, 736

Patterson, J., et al. 1998, PASP, 110, 1290

Patterson, J., et al. 2002, PASP, 114, 721

Patterson, J., et al. 2003, PASP, 115, 1308

Patterson, J., et al. 2005, PASP, 117, 1204

Pavlenko, E., et al. 2007, in ASP Conf. Ser. 372, European Workshop on White Dwarfs, ed. R. Napiwotzki & M. R. Burleigh (San Francisco: ASP), 511

Rolfe, D. J., Abbott, T. M. C., & Haswell, C. A. 2001, in Lecture Notes in Physics 573, Astrotomography, Indirect Imaging Methods in Observational Astronomy, ed. H. M. J. Boffin, D. Steeghs, & J. Cuypers (Berlin: Springer-Verlag), 39

Schlegel, D. J., Finkbeiner, D. P., & Davis, M. 1998, ApJ, 500, 525

Shakura, N. I., & Sunyaev, R. A. 1973, A&A, 24, 337

Skrutskie, M. F., et al. 2006, AJ, 131, 1163

Smak, J. 1982, Acta Astron., 32, 199

Smak, J. 1984, Acta Astron., 34, 161

Smak, J. 2005, Acta Astron., 55, 367

Stellingwerf, R. F. 1978, ApJ, 224, 953

Stolz, B., & Schoembs, R. 1984, A&A, 132, 187

Templeton, M. R., et al. 2006, PASP, 118, 236

Uemura, M., et al. 2002, PASJ, 54, 599

van der Woerd, H., van der Klis, M., van Paradijs, J., Beuermann, K., & Motch, C. 1988, ApJ, 330, 911

Warner, B. 1995b, Ap&SS, 226, 187

Warner, B. 1995a, Cataclysmic Variable Stars (Cambridge: Cambridge University Press)

Warner, B. 1998, in ASP Conf. Ser. 137, Wild Stars in the Old West, ed. S. Howell, E. Kuulkers, & C. Woodward (San Francisco: ASP), 2

Watanabe, M., et al. 2005, PASP, 117, 870

Whitehurst, R. 1988, MNRAS, 232, 35

Williams, R. E. 1980, ApJ, 235, 939